Single Crystalline 4H-SiC Membrane Resonators

Pen-Li Yu*, Noah Opondo, Sen Dai, Boyang Jiang, Dallas T. Morisette and Sunil A. Bhave
School of Electrical and Computer Engineering
Purdue University
West Lafayette, IN 47906, USA
*yu586@purdue.edu

***Abstract*—We report the first wafer-scale fabrication of semi-insulating, single-crystalline 4H-SiC membrane resonators by timed deep reactive ion etch (DRIE). Trenches were etched $184\,\mu m$ deep with 84.7° sidewall angle to form $16\,\mu m$ thick suspended membranes. Sidewall angle, DRIE footing, and surface roughness are characterized. Measured resonance frequencies match with COMSOL simulation within 4%. The modes have quality factors of 500 to 1000 at ambient condition.**

***Index Terms*—Membrane resonator, Single-crystalline 4H-SiC, DRIE**

I. Introduction

Single-crystalline 4H Silicon Carbide (SiC) is an intriguing material with exceptionally low acoustic loss [1]–[3], high stiffness, excellent thermal conductivity, and built-in optically active defects that can be used as spin qubits [4]. A free-standing structure of single crystalline SiC will open applications for harsh environment microelectromechanical systems (MEMS) [5], [6], high-performance filters [7], high-quality-factor MEMS gyroscopes [8-9], and hybrid quantum systems [10], [11].

Traditionally, the free-standing structure is defined by thin film deposition and subsequent removal of the underlying substrate. However, for single crystalline 4H-SiC, this planar approach is not feasible since epitaxial 4H SiC can only be grown on 4H SiC. Smart-cut technique has been demonstrated for 4H-SiC [12], but there are concerns of surface roughness as well as damaging the quantum coherence of the spin states of the defects. To maintain the pristine quality of the resonators top surface, we developed the first wafer-level fabrication of semi-insulating, single-crystalline 4H-SiC membrane micro-resonators by using backside Deep Reactive Ion Etch (DRIE). The etch chemistry allows us to selectively etch $184\,\mu m$ SiC trenches with 84.7° sidewall angles to form $16\,\mu m$ thick membranes. Resonance frequencies up to 5 MHz are measured. Quality factors of 500-1000 at room temperature and atmospheric pressure are found. We highlight the geometric features of the DRIE etched membrane that are important to get thinner and higher-Q 4H-SiC membrane resonators.

II. Fabrication and Characterization

A. Fabrication Process

Fig. 1(a)-(f) presents main process steps for the single crystalline 4H SiC membranes. We use a semi-insulating 4H-SiC wafer with 4-inch diameter and $500\,\mu m$ thickness from Cree Inc. The wafer is $\langle 0001 \rangle$ oriented within 0.2° and has resistivity of $1 \times 10^9\,\Omega \cdot cm$. The fabrication starts with mechanical thinning of the wafer to $200\,\mu m$ [Fig. 1(a)]. In Fig. 1(b)-(d), a lift-off process is employed to get a $2\,\mu m$ Indium Tin Oxide (ITO) DRIE hard mask. $6\,\mu m$ photoresist AZ9260 is applied and patterned on the wafer as the sacrificial stencil layer. $2\,\mu m$ ITO and $20\,nm$ Ti (adhesion layer) are deposited by an electron beam evaporator. The AZ9260 is removed by soaking in $70\,^\circ C$ PG remover for 15 mins. We utilize ITO because it does not react with fluorine ions and is stable under high RIE energies with minimal back-sputtering. In Fig. 1(e), the wafer is mounted on a 6 inch carrier wafer by Crystalbond™and time etched $184\,\mu m$ in Panasonic RIE/ICP etcher using SF_6. The following process parameters are used:

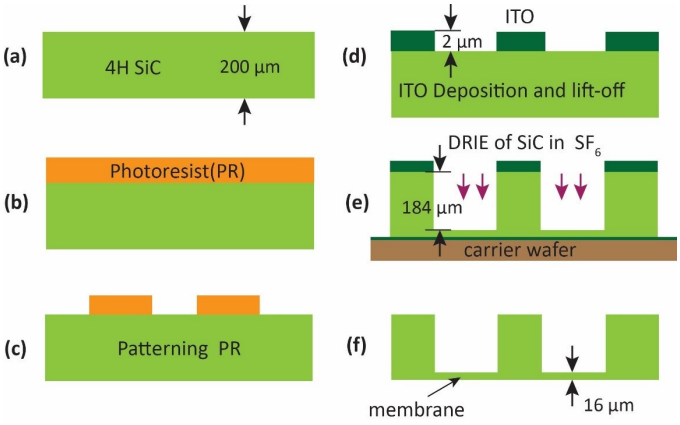

Fig. 1. Fabrication process of single crystalline 4H SiC membrane resonators. See main text for descriptions of each step.

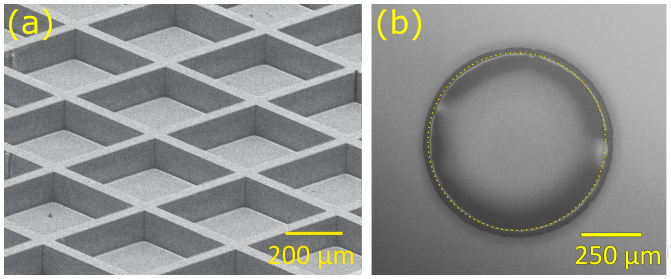

Fig. 2. SEM images of membranes:(a) Square membranes viewed from the etched side. (b) Top view of a circular membrane with $1000\,\mu m$ diameter.

Devices and experiments were supported by the Air Force Office of Scientific Research.

RF power 1150 W, platen power 100 W, pressure 0.8 Pa, and 80 sccm SF_6 flow rate. The etch chemistry is similar to [8] except for the DC bias voltage. We monitor the chamber temperature during the etching. Etching is carried out at intervals of 1 hour to avoid overheating. Etch depth and uniformity are monitored with Bruker GT-K Optical Profilometer after each interval. An etch rate of 12 µm/hour and an ITO:SiC selectivity of 1:146 are achieved. Crystalbond™is chosen over photoresist as the adhesive because its thermal conductivity is better. The carrier wafer was also coated with ITO/Ti to prevent the loading effect and wafer thinning. Fig. 3 shows an example profile when the etch ends. After etching SiC of 186 µm, the SiC wafer and the carrier wafer are soaked in 70 °C hot DI water to dissolve Crystalbond and detach the two wafers. The carbide wafer is then transferred to 70 °C HCl to remove ITO and Ti. Two SEM images of the final devices are shown in Fig. 2.

B. Resonance Characterization

We characterize the membrane resonances with a Polytec MSA-400 scanning Laser Doppler Vibrometer (LDV). The membrane is excited by an axial PZT actuator with a bandwidth of 8 MHz. The PZT is bonded to the edge of the chip to prevent air trapping between the trenches and the PZT. A pseudo-random waveform is applied on the PZT actuator to generate broadband excitation. It is found that our PZT deliver sufficient energy to the membrane up to 6 MHz.The laser is raster scanned to measure the mode shapes. See Fig. 4(a) for the schematic of the experimental setup. Fig. 4(b) shows the average displacement spectrum from 0-5 MHz and the measured mode shape of the membrane shown in Figure 2(b). The measured resonance frequencies match well with COMSOL finite element simulations of the membrane modes, listed in Table I. For the FEM simulation, we construct a circular membrane with a uniform thickness of 16 µm (Fig. 4(c)) and apply a 3D fixed boundary condition to the perimeter. The simulated thickness agrees well with the optical profilometer measurement of DRIE trench.

TABLE I
SIMULATION AND MEASUREMENT OF A 16 µm MEMBRANE'S RESONANCE

Measured Frequency (MHz)	Simulated Frequency (MHz)	Relative Deviation (%)
0.366	0.376	2.57
0.782	0.763	-2.42
1.259	1.251	-0.60
1.476	1.426	-3.38
1.854	1.829	-1.32
2.251	2.181	-3.12
2.477	2.495	0.73
3.100	3.030	-2.25
3.318	3.194	-3.74
4.321	4.299	-0.51
4.835	5.000	3.40
4.996	5.002	0.11

The quality factor (Q) of each mode is obtained by fitting the power spectrum (proportional to the square of the displacement) to a Lorentzian function, as shown in Fig. 4(b).

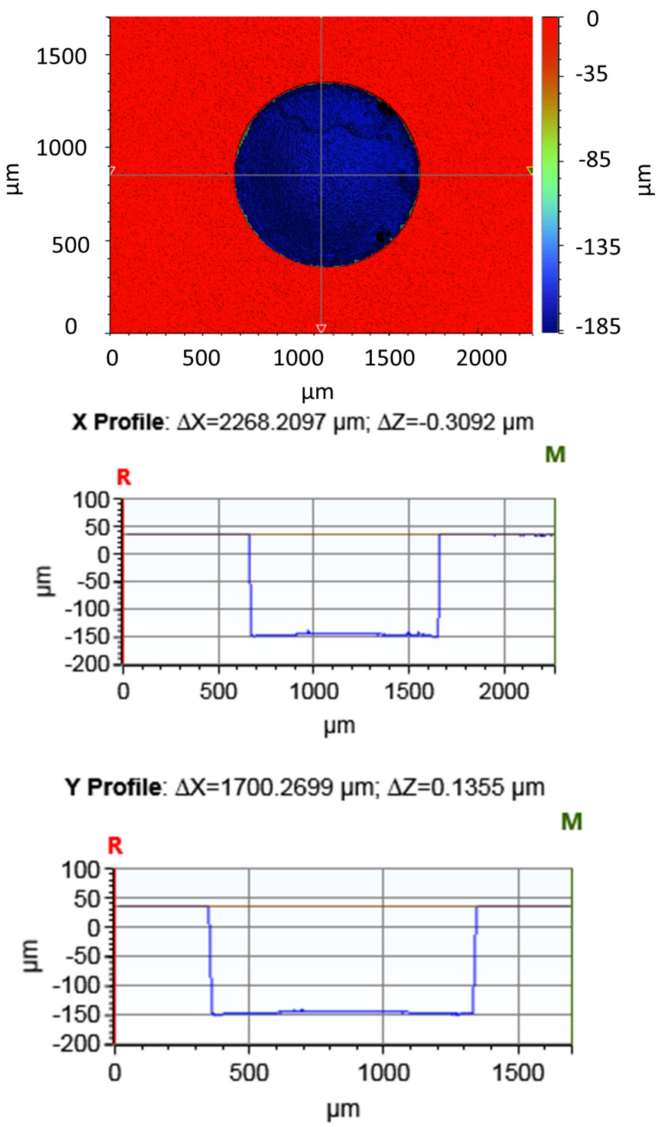

Fig. 3. Optical profilometer measurements of DRIE trench. ContourGT-K 3D Optical Microscope is used to characterize the etch depth. The top graph shows the landscape viewed from the etched side. The color represent the height. The two plots below are the 1D profiles defined by the X and Y direction cut lines in (a), respectively.

The Qs are found to be in the range of 500-1000. The quality factors are the same in both atmosphere pressure and vacuum, indicating that air loss is not the dominant mechanism. Since these membranes are relatively thick and the anchor loss is inversely proportional to the cube of the thickness [13], we attribute the low Q to anchor loss.

III. DISCUSSION

Profilometer and resonance frequency measurements show that membranes with different diameters have different thickness. Although the etch rates only change by 7% from 1000 µm opening to 300 µm opening, the membrane thickness can differ by almost a factor of two, as shown in Fig. 5. Fig. 5(a) plots the etch rate as a function of etch opening.

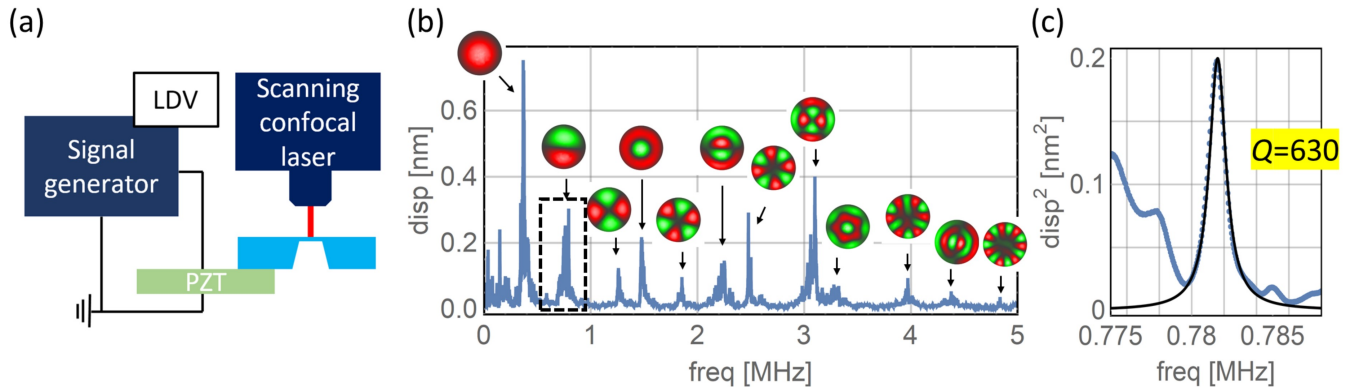

Fig. 4. Resonance mode characterization with Laser Doppler Vibrometer. (a) Schematic of the experimental setup. The membrane device is shown in blue. The PZT actuator is shown in green. (b) Displacement spectrum of the membrane in Fig. 2 measured by the LDV in FFT mode. The mode shapes are mapped by raster-scanning the laser. (c) Zoom in of the spectrum in the dashed box in (a). Q is extracted by fitting the power spectrum (proportional to displacement square) to a Lorentzian function. A quality factor of 630 is obtained for the (1,1) mode at 0.781 MHz at room temperature and atmosphere pressure.

Fig. 5(b) plots the etch depth and the membrane thickness as a function of membrane diameter. The membrane thickness is calculated by subtracting the etch depth from the 200 µm substrate thickness.

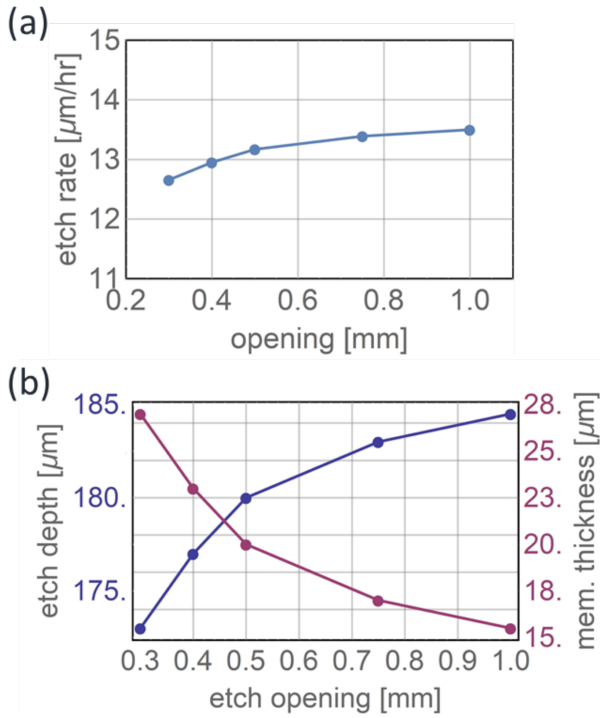

Fig. 5. Summary of etch rate, etch depth, and membrane thickness as a function of etch opening:(a) Etch rate as a function of etch opening. (b) Blue data are the etch depth as a function of etch opening. Red data are the membrane thickness as a function of membrane diameter.

Three DRIE features are crucial to achieve high quality factors: vertical walls, footing, and roughness of the etched surfaces.

The etch recipe realizes 84.7° sidewalls with a continuous single mode operation, without the need to alternate between two modes as in the Bosch process [See Fig. 6(a) and Fig. 7 for examples of the etch sidewall]. To understand the etch mechanism, we perform element analysis with Energy dispersion X-ray Spectroscopy (EDX) on the etched sidewall. We detect Carbon (C), Fluorine (F), and Oxygen (O) [Fig. 6(b)]. These elements indicate a passivated layer of materials such as C_xF_y and SiF_xO_y is formed during the DRIE [8], [15].

Footing is characterized by comparing etch depth at the base of the sidewall to the other areas of the trench. Fig. 7(a) shows the convex nature of the bottom surface. The center of the membrane is 5 µm thicker than the edge of the membrane (500 µm away). In Fig. 7(b), we observe that there is a severe footing effect beneath the sidewall. Micro-trench occurs 20 µm away from the sidewall with a depth a 10 µm. This micro-trench is a result of charging sidewalls which deflect ions toward the base. The passivated layer identified in Fig. 6(b) has a greater tendency to charge than SiC [15].

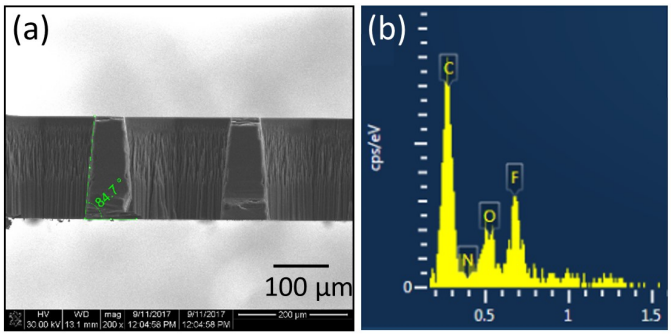

Fig. 6. Sidewall angles and element analysis:(a) SEM images of the cross-section of through DRIE. A sidewall angle of 84.7° is achieved. (b) We analysis the elements of the sidewall surface by performing Energy dispersion X-ray Spectroscopy (EDX). Carbon, Florine, Oxygen are detected. Si is intentionally excluded in this measurement to see the other elements clearly.

Micro-masking is the re-sputtering of the mask material on the etched area during DRIE. These micro-masks results in SiC residues and pillars on the etch surface. Fig. 8(a) shows an optical micrograph of a membrane with micro-masked SiC

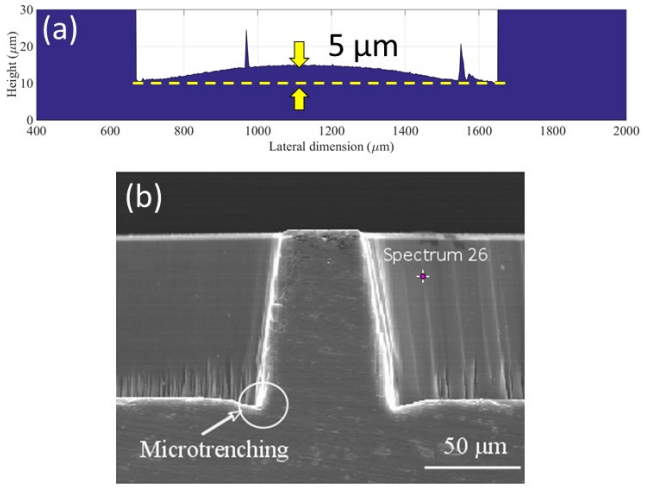

Fig. 7. DRIE footing:(a) Optical profilometer measurement of the DRIE footing (membrane surface). We zoom in to the bottom of the trench to see the convex feature of the membrane. (b) SEM image of the micro-trench beneath the vertical sidewall.

residues. Fig. 8(b) shows two micro-pillars that occur due to micro-masking.

The etched surface quality is analyzed by using Bruker GT-K Optical Profilometer. A roughness average R_a (arithmetical mean deviation) of $4.31\,\mathrm{nm}$ (Fig. 9) is measured at the membrane with negligible micro-masking effect. This level of surface roughness is better than that from mechanical machining [14]. Although the measurement precision is limited by the resolution of profilometer, it confirms that our membrane is of high surface quality and the quality factor is not limited by surface loss.

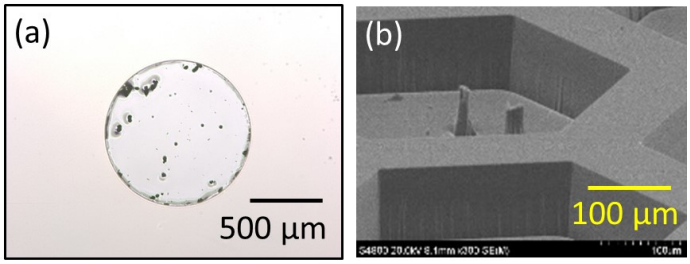

Fig. 8. Micro-masking effect:(a) Optical microscope image of a membrane with micro-masked SiC residues. (b) SEM image of a membrane with micro-masked pillars.

In conclusion, we fabricated the first single crystalline 4H SiC membrane resonators fabrication by DRIE at wafer scale. The resulting membrane surfaces are characterized by SEM and optical profilometer, showing a smooth surface roughness of $4.31\,\mathrm{nm}$. A single-mode DRIE with an etched sidewall angle of $84.7°$ is demonstrated. The mechanical resonances are measured by LDV from 0-5 MHz. Quality factors are 500-1000 at ambient condition. The measured mechanical modes and FEM simulation agrees well, suggesting well-confined resonances and a predictive FEM model. This work paves the way for realizing nanomechanical and nanophtonics devices to interface with coherent spin states in 4H SiC.

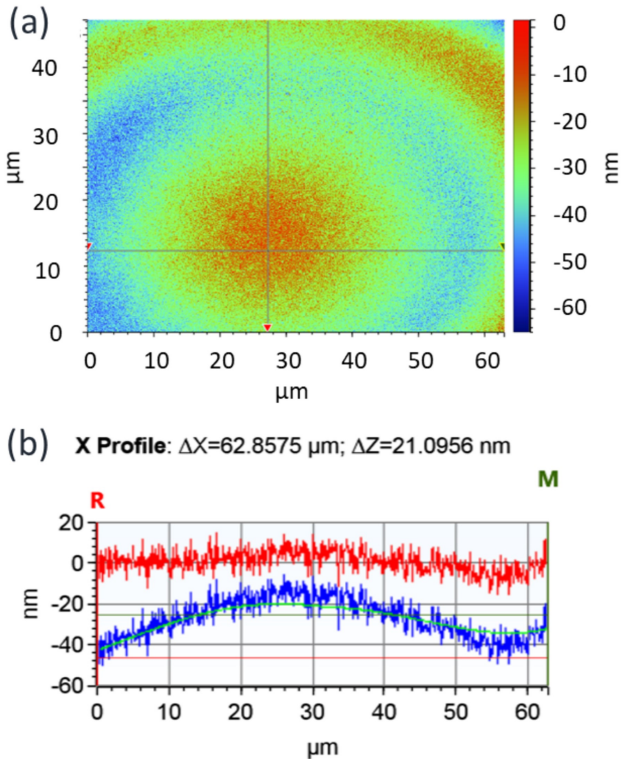

Fig. 9. Measurement of membrane surface roughness:(a) Height heatmap of part of the membrane surface by Bruker GT-K. (b) The X profile of the membrane, cutting along the horizontal line in (a). The blue curve is the measured height, while the green line is second order Gaussian regression fitting applied to eliminate the surface curvature on roughness measurement. The red line shows the difference between the two, which indicates the roughness of the surface.

ACKNOWLEDGMENT

We appreciate S. Reinhart and R. P. Ramamurthy for technical support on the Panasonic E620 Etcher and the EDX measurements, respectively. We thank Mert M. Torunbalci and D. Weinstein for insightful discussions.

REFERENCES

[1] T. A. Gosavi, E. R. Macquarrie, G. D. Fuchs, and S. A. Bhave, HBAR as a High Frequency High Stress Generator, in Ultrasonics Symposium, 2015 IEEE, 2015.

[2] S. Ghaffari, S. A. Chandorkar, S. Wang, E. J. Ng, C. H. Ahn, V. Hong, Y. Yang, and T. W. Kenny, Quantum Limit of Quality Factor in Silicon Micro and Nano Mechanical Resonators, Sci. Rep., vol. 3, p. 3244, Jan. 2013.

[3] J. Yang, B. Hamelin, S.-D. Ko, and F. Ayazi, Ultra-high Q Monocrystalline silicon carbide disk resonators anchored upon a phononoic crystal, 2018 Solid State Sensor, Actuator and Microsystems Workshop (Hilton Head 2018), Hilton Head Island, South Carolina, June 3-7, 2018.

[4] W. F. Koehl, B. B. Buckley, F. J. Heremans, G. Calusine, and D. D. Awschalom, Room temperature coherent control of defect spin qubits in silicon carbide, Nat., vol. 479, no. 7371, p. 84, 2011.

[5] M. Mehregany, C. A. Zorman, N. Rajan, and C. H. Wu, Silicon carbide MEMS for harsh environments, Proc. IEEE, vol. 86, no. 8, pp. 15941609, Aug. 1998.

[6] J. B. Shealy, R. Vetury, S. R. Gibb, M. D. Hodge, P. Patel, M. A. McLain, A. Y. Feldman, M. D. Boomgarden, M. P. Lewis, B. Hosse, and R. Holden, Low loss, 3.7GHz wideband BAW filters, using high power single crystal AlN-on-SiC resonators, in 2017 IEEE MTT-S International Microwave Symposium (IMS), 2017, pp. 14761479.

[7] R. Perahia, L.D. Sorenson, J.L. Bregman, L.X. Huang, M.S. White, K.S. Holabird, and D.T. Chang, Piezoelectric single crystal 6H Silicon carbide microelectromechanical resonators, 2018 Solid State Sensor, Actuator and Microsystems Workshop (Hilton Head 2018), Hilton Head Island, South Carolina, June 3-7, 2018.

[8] S. Ko, B. Hamelin, J. Yang, and F. Ayazi, High-Q Monocrystalline Silicon Carbide Disk Resonators Fabricated Using DRIE Of Thick SiC-on-Insulator Substrates, in MEMS, 2018, no. January, pp. 996999.

[9] E. Cook, M. Tomaino-Iannucci, J. Bernstein, M. Weinberg, J. Choy, K. Hobart, L. Luna, M. Tadjer, R. Myers-Ward, F. Kub, Y. Yang, E. Ng, I. Flader, Y. Chen, and T. Kenny, A High-mass, eight-fold Symmetric Silicon Carbide MEMS Gyroscope, 2018 Solid State Sensor, Actuator and Microsystems Workshop (Hilton Head 2018), Hilton Head Island, South Carolina, June 3-7, 2018.

[10] S. J. Whiteley, G. Wolfowicz, C. P. Anderson, A. Bourassa, H. Ma, M. Ye, G. Koolstra, K. J. Satzingfer, M. V. Holt, F. J. Heremans, A. N. Cleland, D. I. Schuster, G. Galli, and D. D. Awschalom, Coherent Control of Spins with Gaussian Acoustics, in arxiv: 1804.10996 [quant-ph].

[11] P.-L. Yu, T. P. Purdy, and C. A. Regal, Control of Material Damping in High-Q Membrane Microresonators, Phys. Rev. Lett., vol. 108, no. 8, pp. 083603, 2012.

[12] J.-H. Lee, I. Bargatin, J. Park, K. M. Milanina, L S. Theogarajan, R. Sinclair, and R. T. Howe, Smart-cut layer transfer of single-crystal SiC using spin-on-glass, J. Vac. Sci. Technol., vol. 30, no. 4, p. 042001, 2012.

[13] K. K. Park, H. J. Lee, P. Crisman, M. Kupnik, . Oralkan, and B. T. Khuri-Yakub, "Optimum design of circular CMUT membranes for high quality factor in air," in Ultrasonics Symposium, 2008 IEEE, 2008.

[14] Goel, Saurav, et al. "Brittleductile transition during diamond turning of single crystal silicon carbide," International Journal of Machine Tools and Manufacture 65 (2013): 15-21.

[15] Glenn M. Beheim, and Laura J. Evans, Control of Trenching and Surface Roughness in Deep Reactive Ion Etched 4H and 6H SiC, Mater. Res. Soc. Symp. Proc. 2006; 910: B10.